Nanoparticle induced self-assembly

2008 J. Phys.: Condens. Matter 20 204127

(http://iopscience.iop.org/0953-8984/20/20/204127)

IOP Publishing Journal of Physics: Condensed Matter

J. Phys.: Condens. Matter **20** (2008) 204127 (6pp) doi:10.1088/0953-8984/20/20/204127

Nanoparticle induced self-assembly

G Helgesen[1], E Svåsand[1,2] and A T Skjeltorp[1,2]

[1] Physics Department, Institute for Energy Technology, NO-2027 Kjeller, Norway
[2] Department of Physics, University of Oslo, NO-0316 Oslo, Norway

Received 1 April 2008
Published 1 May 2008
Online at stacks.iop.org/JPhysCM/20/204127

Abstract

Self-assembly has for the large part focused on the assembly of molecules without guidance or management from an outside source. However, self-assembly is in principle by no means limited to molecules or the nanoscale. A particularly interesting method to the self-assembly of micro- to millimetre sized components is the use of the 'magnetic hole' effect. In this method, nonmagnetic particles can be manipulated by external magnetic fields by immersing them in a dispersion of colloidal, magnetic nanoparticles, denoted ferrofluids. Nonmagnetic particles in magnetized ferrofluids are in many ways ideal model systems to test various forms of particle self-assembly and dynamics. When microspheres are confined to a monolayer between two parallel plates and subjected to static or oscillating magnetic fields they show a variety of dynamical behaviours and assemblages, depending on the frequency and direction of the external fields. A single pair of magnetic holes oscillating in a ferrofluid layer may be used to measure the viscosity of tiny volumes of the fluid. We have also observed ordering of dilute dispersions of macromolecules and nanoparticles in magnetized ferrofluids. The self-assembly at this length scale results from structural correlations between these nanostructures and ferrofluid particles rather than from the macroscopic magnetostatic effect for the magnetic holes.

(Some figures in this article are in colour only in the electronic version)

1. Introduction

Monodisperse polystyrene spheres [1] dispersed in ferrofluid[3] provide a convenient model system for the study of various order–disorder phenomena. The basis for this is that the spheres displace the ferrofluid and behave as magnetic holes with effective moments equal to the total moment of the displaced fluid [2]. The spheres are much larger (1–100 μm) than the magnetic particles (typically 10 nm) in the ferrofluid. The spheres therefore move around in an approximately homogeneous magnetic background. For microspheres of diameter >10 μm the thermal motion is negligible and the only forces which have to be taken into consideration are the viscous and magnetic forces.

By confining the spheres and ferrofluid between closely spaced microscope slides, an essentially two-dimensional many-body system of interacting particles is obtained. This offers the possibility of observing, directly through a microscope, a wide range of nonlinear dynamic phenomena and collective processes, as magnetic holes are easy to produce and to manipulate with external magnetic fields. A simplifying feature of magnetic holes is that their magnetic moments are collinear with an external field at any field strength. This is in contrast with magnetic particles dispersed in nonmagnetic fluids where random orientation of the magnetic moments complicates the theoretical treatment of the dynamic and static properties of the system.

[3] Ferrotec GmbH, Hohes Gestade 14, 72622 Nürtingen, Germany.

2. Interactions of magnetic holes

The basic principle for magnetic holes is shown in figure 1. It is in some sense a magnetic analogue of Archimedes' principle. When a nonmagnetic, spherical particle is dispersed in a magnetized ferrofluid with a magnetic field $H > 0$, the void produced by the particle possesses an effective magnetic moment M_V equal in size, but opposite in direction, to the magnetic moment of the displaced fluid

$$M_V = V\chi_{\text{eff}}H, \quad \text{with } \chi_{\text{eff}} = 3\chi/(3+2\chi), \tag{1}$$

where V is the volume of the sphere, χ_{eff} is the effective susceptibility, and χ is the volume susceptibility of the ferrofluid. The interaction energy between two spheres with

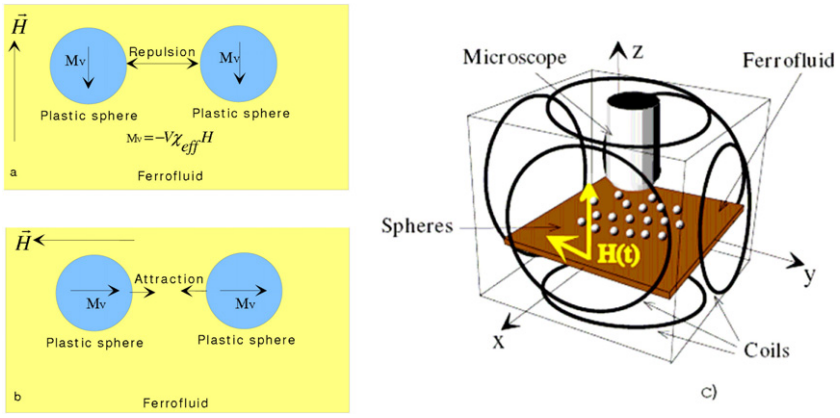

Figure 1. The principle of a magnetic hole in a ferrofluid; (a) two holes side by side will repel each other and (b) two holes with their centres collinear with the field lines will attract each other. (c) The experimental setup with coil pairs along the x-, y-, and z-directions.

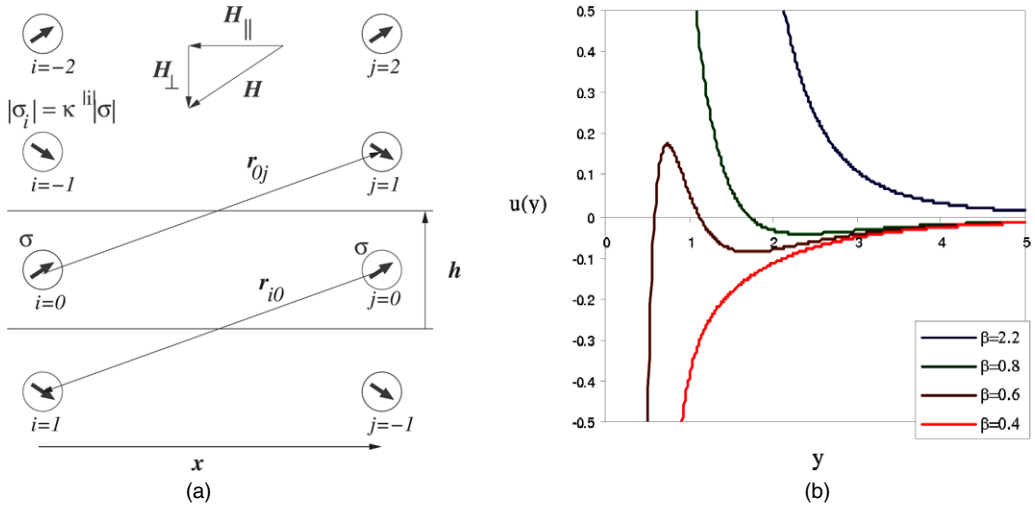

Figure 2. (a) Pair of nonmagnetic spheres in a ferrofluid layer, viewed along the confinement plates, and the series of dipole images accounting for the boundary conditions of the magnetic field along the plates. (b) The pair potential u versus dimensionless particle separation $y = x/h$, equation (4), for some values of the field component ratio β.

a centre-to-centre separation r is given approximately by the dipolar interaction [2]

$$U \propto \frac{M_V^2(1-3\cos^2\theta)}{r^3}. \tag{2}$$

Here, θ is the angle between the line connecting the centres of the spheres and the direction of the field.

The susceptibility contrast between the ferrofluid and the two plane nonmagnetic confining plates leads to a deviation from the purely dipolar interaction of equation (2). According to the image method, the boundary conditions for the magnetic field along the plates are fulfilled with the addition of an infinite series of dipole images σ_i to the expression for the interaction in an unbounded medium. The images are constructed as mirror images in the plane boundaries of the initial dipoles $\sigma_0 = M_V$ or of some previous image, multiplying the magnitude of the dipole at each mirror symmetry operation by an attenuation factor $\kappa = \chi/(\chi+2)$ as shown in figure 2(a) [3].

The instantaneous interaction potential between a pair of confined holes can then, similarly to equation (2), be expressed as

$$U = \frac{\mu}{8\pi}\sum_{i\neq j}\left[\frac{\vec{\sigma}_i\cdot\vec{\sigma}_j}{r_{ij}^3} - 3\frac{(\vec{\sigma}_i\cdot\vec{r}_{ij})(\vec{\sigma}_j\cdot\vec{r}_{ij})}{r_{ij}^5}\right], \tag{3}$$

where $\mu = \mu_0(1+\chi)$ is the ferrofluid's permeability and $\mu_0 = 4\pi \times 10^{-7}$ H m^{-1}. The i-index runs over both the source and image dipoles and the j-index runs only over the two source dipoles. A detailed analysis of the equation above shows that the dominant effect for the force components normal to the plates is the interaction between a particle and its own mirror image, which stabilizes the particles midway between the plates.

Decomposing the instantaneous field in its in-plane $\mathbf{H}_\perp$ and normal $\mathbf{H}_\parallel$ components, we denote the ratio of their magnitudes as $\beta = H_\perp/H_\parallel$, the sphere diameter a, plate separation h, and the scaled horizontal separation as $y = x/h$. Using a magnetic field that is rotating in the x–y plane with a frequency $f = 10$–100 Hz (which exceeds the inverse viscous relaxation time $f_c = \mu\chi_{\text{eff}}^2 H_\parallel^2/(1152\pi\eta)$), the relative motion

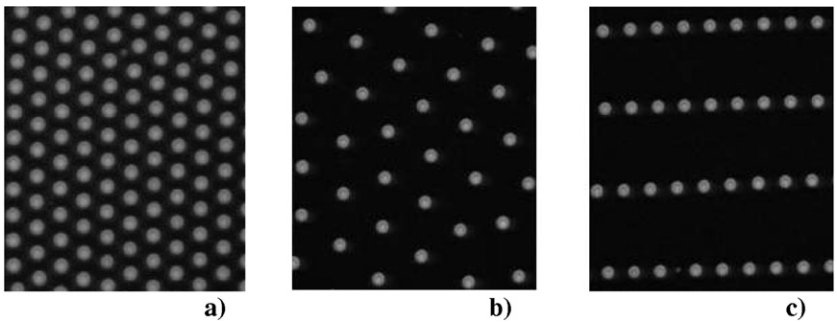

Figure 3. Typical static structures of magnetic holes formed for $H_x = 800$ A m^{-1}. (a) $\beta = 0.3$, $\varepsilon = 0$, (b) $\beta = 1.5$, $\varepsilon = 0.44$, and (c) $\beta = 1.5$, $\varepsilon = 0.87$.

of the holes can be neglected during one rotation of the field, and an effective, time-averaged interaction potential can be obtained by averaging over a full rotation of the magnetic field. This leads to the following dimensionless form of the time-averaged, effective interaction potential $\overline{U(\frac{x}{h})}$ [3]

$$u(y) \equiv \frac{144h^3\overline{U(y)}}{\mu\pi a^6\chi_{\text{eff}}^2 H_\parallel^2} = \sum_{l=-\infty}^{+\infty} \kappa^{|l|}\left[\frac{1+(-1)^{|l|}\beta^2}{(y^2+l^2)^{3/2}} - 3\frac{(-1)^{|l|}l^2\beta^2 + y^2/2}{(y^2+l^2)^{5/2}}\right]. \quad (4)$$

The term $l = 0$ corresponds to the source–source interaction term, the others to interactions between a particle and the images of the other ones.

For the micrometre sized spheres used here, the Reynolds number is very low and inertial terms can then be neglected, and the magnetic forces are balanced by the viscous Stokes force given by

$$F_{\text{visc}} = 3\pi\eta_{\text{a}} a v, \quad (5)$$

where η_{a} is an apparent fluid viscosity (equal to the bulk viscosity in an unbounded medium) and v is the velocity of the sphere. Thus, the static structures as well as the dynamics of microsphere motion can be calculated, and these calculations are in good quantitative agreement with experiments [3, 4].

3. Experiments on microspheres

By adjusting the ratio $\beta = H_\perp/H_\parallel$, it is possible to tune the pair interaction potential from purely repulsive for small values of β, via metastable and stable fixed particle separations with $x > a$ for intermediate β-values, to a purely repulsive potential for large β. This is illustrated in figures 3(a), (b) and gives rise to triangular lattices with a tunable particle separation. However, it is also possible to introduce asymmetry in the rotating in-plane component $H_\parallel = \sqrt{H_x^2 + H_y^2}$ with $\varepsilon = H_y/H_x < 1$, thus having an elliptically polarized field. Such fields give rise to triangular or rectangular lattices with two separate continuously tunable lattice parameters as shown in figure 3(c).

By using smaller spheres, typically $a \leqslant 2$ μm, it is possible to reduce the particle interactions to a magnitude comparable to thermal forces and energies, and Brownian motions of the microspheres become visible. Then the controlling parameter for the stability of the structure formation is the ratio of the dipolar energy to the thermal energy $\Gamma = M_V^2/(d^3 k_{\text{B}} T)$, where d is the typical centre-to-centre separation of the spheres, k_{B} is Boltzmann's constant and T is the temperature. Values of Γ from about 8 up to several thousand can be reached.

As we were using a rotating magnetic field *perpendicular* to the x–y sample plane, i.e. (H_x, H_z), and only two nearby spheres of typical size $a = 50$ μm in the sample cell, it was possible to set the spheres in stable oscillations with no direct contact between their surfaces [5]. The magnitude of the field was about 2 kA m^{-1}, rotation frequency 0.05 Hz, and the plate separation was $h = 2a$. This oscillating motion was stable for more than half an hour. This setup can be used to measure the viscosity of the fluid because both magnetic and viscous forces can be calculated.

Since the plate separation in this experiment is comparable to the sphere diameter, there is an increased viscous drag on the spheres induced by the walls, and the viscosity η_{a} seems to be higher than the bulk viscosity η_0 [7].

$$\frac{\eta_{\text{a}}}{\eta_0} = 2\left(1 - \frac{9}{16}\left(\frac{a}{h}\right) + \frac{1}{8}\left(\frac{a}{h}\right)^3 - \frac{45}{256}\left(\frac{a}{h}\right)^4 - \frac{1}{16}\left(\frac{a}{h}\right)^5\right)^{-1} - 1. \quad (6)$$

In a similar way, the second sphere will give rise to an increased drag on the first sphere. This effect has been calculated [6] and for equal spheres that are not very close, the increase in the viscosity, as manifested by an apparent viscosity η_{a}, is given by

$$\frac{\eta_{\text{a}}}{\eta_0} = \left(1 - \frac{3}{4}\left(\frac{a}{x}\right) + \frac{1}{8}\left(\frac{a}{x}\right)^3 - \frac{15}{64}\left(\frac{a}{x}\right)^4\right)^{-1}. \quad (7)$$

The correction factors of equations (6) and (7) are plotted in figure 4(a) and are important even for plate separation h/a and sphere separation x/a as large as 6.

When the two spheres are close, they may partly screen the external applied magnetic field for each other. In order to be sure that the sphere separation in these experiments was sufficient such that the effective susceptibility is well approximated by the expression given in equation (1), we performed a numerical calculation of the effective

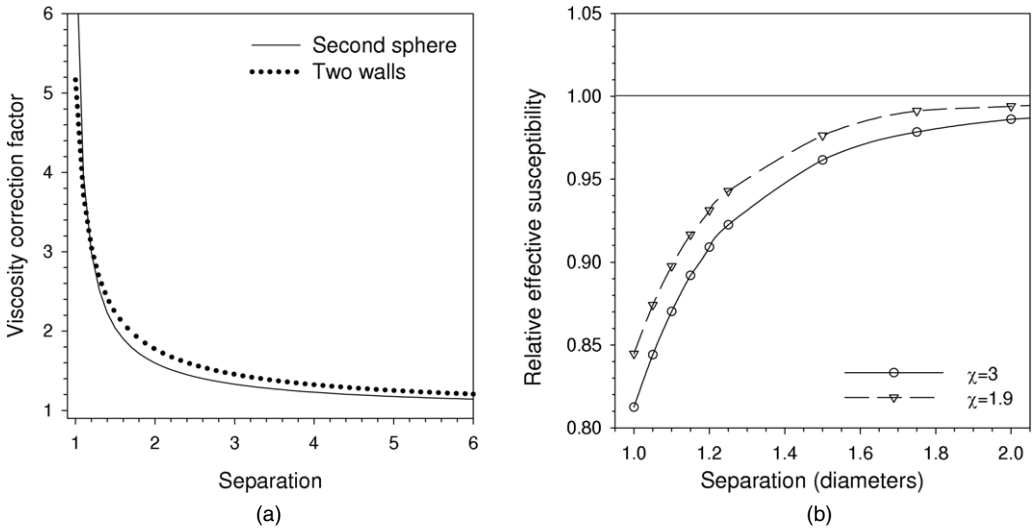

Figure 4. (a) Viscosity correction factor η_a/η_0 for two spheres at a separation x/a (a = sphere diameter) moving toward each other (solid line) and for a sphere moving in the centre between two plates with separation h/a. (b) The effective susceptibility of a sphere relative to the first order approximation $\chi_{\text{eff}} = 3\chi/(3+2\chi)$ for two spheres in a parallel field separated by centre-to-centre distance x/a.

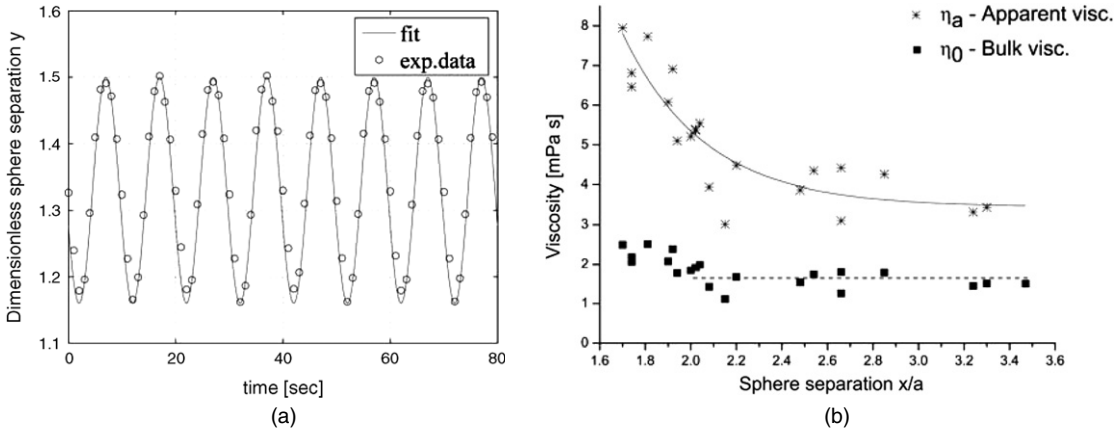

Figure 5. (a) Separation distance of two magnetic holes versus time for a setup with the magnetic field rotating at $f = 0.05$ Hz in the x–z plane. (b) Apparent viscosity and bulk viscosity for a commercial ferrofluid versus separation of the spheres. The solid line is a guide to the eye and the dashed line shows the mean value for $x/a > 2$.

susceptibility χ_{eff} as a function of the sphere centre-to-centre separation x for the parallel field configuration shown in figure 1(b). The calculation was done using commercial, finite-element-method software [8], solving the partial differential equations with the proper boundary conditions. Figure 4(b) shows the ratio of the effective susceptibility χ_{eff} to that of the magnetic holes model given in equation (1). For sphere separations larger than about $x/a > 2$ the deviation is less than 2% and thus negligible compared to other effects.

By taking proper account of both the viscous correction effects described above, we have successfully managed to measure the bulk viscosity [5] of a commercial ferrofluid[4]. This is illustrated in figure 5(a) which shows the separation of the spheres (circles—in units of plate separation $h = 2a$) and a fitted sinusoidal curve (solid line). Figure 5(b) shows the apparent viscosity (upper curve) and the bulk viscosity found after correcting for the drag effects in equations (6) and (7). The value we found was consistent with that provided by the producer which was given for a temperature different from that used in our experiment. The great advantage of this method compared to conventional rheometry methods is the tiny volume of fluid that is needed, typically less than 1 μl.

[4] EMG905 from Ferrotec GmbH, with susceptibility $\chi = 1.9$.

4. Self-assembly in binary mixtures of nanoparticles

When the nonmagnetic particle is reduced from micrometre size to nanometre size and its volume becomes comparable to the mean volume occupied by a ferrofluid particle, the concept of an effective magnetic moment for the nonmagnetic species is no longer valid. The first attempts to look for orientation of nanosized biological assemblies in ferrofluids took place at the Institute Laue Langevin (ILL) [9] and somewhat surprisingly, rather strong anisotropic scattering was observed. In these first

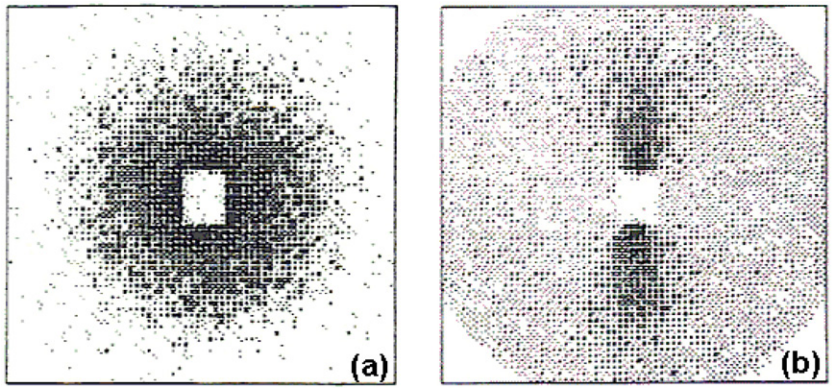

Figure 6. Blank-subtracted SANS scattering intensity patterns from a dispersion of λ-phage in a ferrofluid for (a) $H = 0$ and (b) $H = 240$ kA m^{-1}.

studies λ-phage was used. This is a virus with a spherical head of diameter approximately 50 nm and with a cylindrical tail of length approximately 150 nm. Figure 6 shows small-angle neutron scattering (SANS) data from a dispersion of λ-phage in a ferrofluid with a saturation magnetization of 0.037 T exposed to a magnetic field of 240 kA m^{-1}. There is clearly a pronounced anisotropy due to the alignment of the λ-phage for the blank-subtracted scattered intensity patterns of the dispersion before and after exposure to the magnetic field.

Following these initial studies, some SANS experiments [10] were made on tobacco mosaic virus (TMV), which is a hollow cylindrical assembly of length 300 nm, external diameter 18 nm, and internal diameter 4 nm. Again, a distinct alignment of the TMV in the ferrofluid was observed.

To explain this unexpected behaviour, it is necessary to understand the correlations which may develop in a mixed fluid in which two species of particles coexist. An expression for the scattering from a binary fluid of nonmagnetic spheres has been given by Ashcroft and Langreth [11]. The extension to neutron scattering by a mixture containing a magnetic species is provided by the analysis of Moon *et al* [12]. The scattering of a mixture of nonmagnetic particles and magnetic particles subjected to a magnetic field can thus be modelled to involve three correlation terms: between the magnetic and nonmagnetic particles; between the nonmagnetic particles; and between the magnetic particles. The results show that, for typical densities and dipole strengths, the pair probability distributions of each individual type of particle are relatively unperturbed by the presence of the other species. This means that the ferrofluid particles form chains, much as if the nonmagnetic particles are not present, while the latter find sufficient room between the chains to act as if the ferrofluid is not present. Due to this type of coexistence, very strong cross-correlations between different types of particles can develop in the system. This means that a ferrofluid particle can expect to have another ferrofluid particle as a neighbour in the direction of the field, but most likely a nonmagnetic particle as a neighbour perpendicular to the field, because that is where it has to fit into the dispersion. A series of experiments provided quantitative proof that it is these cross-correlations which determine the anisotropy of the scattering. This was achieved using latex spheres dispersed in ferrofluid, and having contrast variation by selective protonation/deuteration of surfactants and solvents to isolate different terms in the scattering. To our knowledge, it has not been possible to extend the theory for spherical particles outlined here to mixtures of non-spherical particles. However, it is likely that these cross-correlations are also important in achieving structural order in dilute suspensions of mixed magnetic and nonmagnetic colloidal particles of any shape, as demonstrated by the λ-phage and TMV experiments discussed above.

The method outlined here may thus be used to align anisotropic macromolecules and a variety of colloidal nanoparticles in suspension for diffraction measurements. The ability to work with low concentrations makes the method of particular interest for aligning biological materials, such as chromatin, which are not easily obtainable in quantity, and biopolymers, which are not amenable to conventional high-field or shear alignment. Application of this method to scattering experiments eliminates partially the loss of structural information usually inherent in orientational averaging of the molecular form factor. It may also have interesting possibilities for nanoengineering in general, especially when combined with field gradient techniques.

5. Conclusions

In this paper we have shown that the magnetic hole effect can be used to manipulate and induce self-assembly of nonmagnetic microparticles by external magnetic fields. Static structures as well as the dynamics of particle motion are influenced by the boundaries, the degree of confinement, and the direction of the magnetic field. For suspended nanoparticles in ferrofluid, the reason for the alignment effects changes and is more difficult to calculate quantitatively. However, this method may be useful for aligning nanoparticles and biomolecules for further diffraction studies.

Acknowledgments

We thank J Akselvoll, K d L Kristiansen, R Toussaint, E G Flekkøy, and R Pynn for help and useful discussions.

E Svåsand acknowledges the Nanomat program of the Research Council of Norway for support.

References

[1] Ugelstad J, Mørk P C, Kaggerud K H, Ellingsen T and Berge A 1980 *Adv. Colloid Interface Sci.* **13** 101
[2] Skjeltorp A T 1983 *Phys. Rev. Lett.* **51** 2306
[3] Toussaint R, Akselvoll J, Helgesen G, Skjeltorp A T and Flekkøy E G 2004 *Phys. Rev.* E **69** 011407
[4] Kristiansen K d L, Helgesen G and Skjeltorp A T 2006 *Eur. Phys. J.* B **51** 363
[5] Svåsand E, Skjeltorp A T, Akselvoll J and Helgesen G 2006 *J. Appl. Phys.* **101** 054910
[6] Kim S and Karrila S J 2005 *Microhydrodynamics Principles and Selected Applications* (New York: Dover)
[7] Faucheux L P and Libchaber A J 1994 *Phys. Rev.* E **49** 5158
[8] FlexPDE from PDE Solutions Inc., PO Box 609 Sunol, CA 94586 www.pdesolutions.com
[9] Charles S W, Hayter J B, Pynn R and Skjeltorp A T 1984 *Institute Laue Langevin Experimental Report* Grenoble p 251
[10] Hayter J B, Pynn R, Charles S W, Skjeltorp A T, Trewhella J, Stubbs G and Timmins P 1989 *Phys. Rev. Lett.* **62** 1667
[11] Ashcroft N W and Langreth D C 1967 *Phys. Rev.* **156** 685
[12] Moon R M, Riste T and Koehler W C 1969 *Phys. Rev.* **181** 920